Journal Pre-proof

Ratiometric Electrogenerated Chemiluminescence Sensor Based on a Designed Anti-fouling Peptide for the Detection of Carcinoembryonic Antigen

Qiuxia Hao, Lei Wang, Shuyan Niu, Caifeng Ding, Xiliang Luo

PII: S0003-2670(20)30960-0

DOI: https://doi.org/10.1016/j.aca.2020.09.033

Reference: ACA 237972

To appear in: *Analytica Chimica Acta*

Received Date: 23 June 2020

Revised Date: 15 September 2020

Accepted Date: 17 September 2020

Please cite this article as: Q. Hao, L. Wang, S. Niu, C. Ding, X. Luo, Ratiometric Electrogenerated Chemiluminescence Sensor Based on a Designed Anti-fouling Peptide for the Detection of Carcinoembryonic Antigen, *Analytica Chimica Acta*, https://doi.org/10.1016/j.aca.2020.09.033.

Qiuxia Hao: Data curation, Formal analysis, Investigation, Methodology.
Lei Wang: Data curation, Formal analysis, Investigation, Methodology.
Shuyan Niu: Investigation, Validation, Supervision.
Caifeng Ding: Conceptualization, Supervision, Validation, Visualization, Writing - original draft.
Xiliang Luo: Conceptualization, Writing - review & editing.

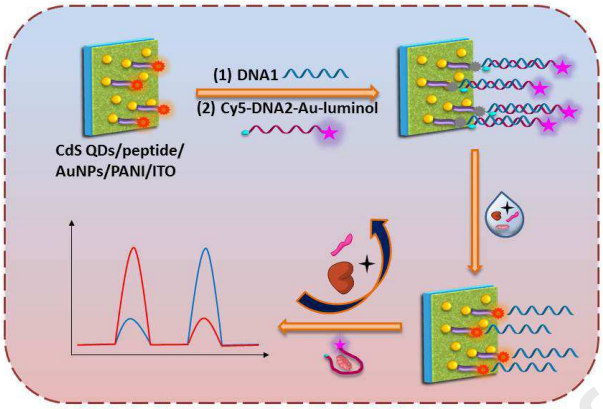

In this paper, an effective and accurate ratiometric electrochemiluminescence (ECL) system based on designed anti-fouling peptide was constructed for detecting carcinoembryonic antigens (CEA) in complex samples with high selectivity and good sensitivity.

Ratiometric Electrogenerated Chemiluminescence Sensor Based on a Designed Anti-fouling Peptide for the Detection of Carcinoembryonic Antigen

Qiuxia Hao, Lei Wang, Shuyan Niu, Caifeng Ding*, Xiliang Luo*

Key Laboratory of Optic-electric Sensing and Analytical Chemistry for Life Science, Ministry of Education; Shandong Key Laboratory of Biochemical Analysis; Key Laboratory of Analytical Chemistry for Life Science in Universities of Shandong; College of Chemistry and Molecular Engineering, Qingdao University of Science and Technology, Qingdao 266042, PR China.

Abstract

In this paper, an effective and accurate ratiometric electrochemiluminescence (ECL) system based on Au-luminol and CdS quantum dots (CdS QDs) as signal probes was constructed for detecting carcinoembryonic antigen (CEA). Polyaniline (PANI) and gold nanoparticles (AuNPs) strongly enhanced the electronic transfer efficiency and the specific area of the modified sensing surface, and improved the detection sensitivity. CdS QDs functionalized DNA strands functioned as cathode ECL emitters, and the aptamer of CEA modified with Au-luminol and quencher cyanine dye (Cy5) fluorophore functioned as anode ECL emitters. After the DNA capture probe combined with CEA aptamer, the negative potential ECL response of the CdS QDs was quenched because of electrochemiluminescence resonance energy transfer (ERET) between the Cy5 fluorophore and CdS QDs. However, the positive potential ECL response of Au-luminol can still be detected. The negative potential ECL response of CdS QDs was recovered, and the positive potential ECL response of Au-luminol decreased after CEA combined with its aptamer to take Cy5 and Au-luminol off the sensing interface. Additionally, the peptide provided effective anti-fouling performance in the detection of complex samples. The ratiometric ECL sensor with anti-fouling ability can sensitively determine the concentration of CEA in human serum.

Keywords: Electrogenerated Chemiluminescence (ECL), Anti-fouling Peptide, Ratiometric Biosensor, Carcinoembryonic Antigen, Au-luminol, CdS QDs

Introduction

Cancer poses a serious threat to human health, second only to heart disease, and can lead to high mortality.[1,2] The early detection of cancer can prolong the lives of cancer patients.[3,4] Carcinoembryonic antigen (CEA), a glycoprotein produced by human tumor cells, is a key cancer biomarker in clinical diagnosis and treatment.[5,6] The formation of many tumors in the human body often leads to high levels of CEA expression.[7] Many reports have claimed that serum CEA levels are significantly higher in some cancer patients, such as those with colon cancer.[8] Consequently, the sensitive determination of CEA has been of high interest to scientists. Thus far, many strategies for analyzing the CEA content have been reported,[9-11] for example, fluorescence immunoassay (FIA),[12-14] inductively coupled plasma mass spectrometry (ICPMS),[15,16] photochemical (PEC) analysis,[17] chemiluminescence analysis,[18-20] enzyme-linked immunoassay (ELISA),[21-23] electrochemical analysis,[24,25] and surface-enhanced Raman scattering (SERS).[26,27]

Electrochemiluminescence (ECL) is a chemiluminescence initiated by an electrochemical stimulus. Different from fluorescence, ECL does not need an external light source but instead excites the luminescent substance by applying the electrode potential to produce chemiluminescence. During ECL analysis, false positive or negative signals are inevitable due to instrumental or environmental factors for a single signal-based strategy. The dual-signal ratiometric technique can eliminate external interference and improve the reliability of detection. As a powerful analytical technique, ECL has the advantages of controllability, low operational difficulty and low background compared with traditional analytical methods and has great development prospects in sensing analysis.[28-32] However, many biosensors will face an extremely

serious challenge in the actual detection, that is, the sensor interface in the complex matrix will greatly impair the performance of the sensor because of the nonspecific adsorption of proteins. To reduce the strong nonspecific attachment of contaminants to the sensing interface, the development of an anti-fouling sensing surface modified with anti-fouling materials, such as polyethylene glycol (PEG) polymers,[33-35] amphoteric polymers,[36-38] and peptide,[39-44] has been attempted. Recently, some strategies using nanoporous gold[45] or silica films[46] for detection in complex real samples have also been reported. Among these materials, the peptide composed of natural amino acids, which has good biocompatibility, has become a potential anti-fouling candidate material with great application potential.[47]

Compared with the single signal detection method, the results of the ratio-based signal detection method in the variable complex external environment are more accurate, and the interference is eliminated by self-tuning the two emissions.[48] Over the past 20 years, Au-luminol and CdS QDs have been widely used in the field of biochemical analysis sensing because of their remarkable advantages in electrochemical reactions.[49] Our group has previously reported several works based on ratio-type signals in which the sensitivity and accuracy of detection have been greatly improved.[50-52]

Based on the above research progress, this paper introduces a ratiometric ECL biosensor based on anti-fouling peptide for the ultrasensitive determination of CEA. The system uses Au-luminol for the positive potential ECL and CdS QDs for the negative potential ECL. CEA was determined according to the ratiometric ECL signal at two different excitation potentials. The ratiometric ECL biosensor is expected to provide a sensitive and reliable analytical strategy for clinical diagnosis and biosensing development in the future.

EXPERIMENTAL SECTION

Reagents and Materials. Chloroauric acid ($HAuCl_4$), chromium chloride ($CdCl_2$), aniline, mercaptopropionic acid (MPA), thioacetamide, luminol, fetal bovine serum (FBS), bovine serum albumin (BSA), N-hydroxysulfosuccinimide sodium salt (NHS), 1-ethyl-3-(3-(dimethylamino)propyl) carbodiimide (EDC), sulfuric acid (H_2SO_4, 95.0-98.0%), sodium hydroxide (NaOH), hydrogen peroxide (H_2O_2, 30%), potassium persulfate ($K_2S_2O_8$), thrombin glucose, hemoglobin, uric acid, and human alpha fetoprotein (AFP) were obtained from Sigma-Aldrich. An indium tin oxide (ITO) coated glass slide was obtained from NanoSci Inc. (China). Raw cells and HeLa cells were obtained from the KeyGEN BioTECH Co. (China). Tris(2-carboxyethyl) phosphine hydrochloride (TCEP), DNA oligonucleotides, CEA and peptide were obtained from the Sangon Biological Engineering Technology & Services Co. (Shanghai, China). The sequences of the peptide, DNA1 (complementary) and DNA2 (aptamer of CEA) strands are as follows:

DKDKDKDPPPPC

5’-AATTGAATAAGCACCCCCTTTTTT-$(CH_2)_6$-NH_2-3’(DNA1)

5’-Cy5-TATCCAGCTTATTCAATTTTTTTT-$(CH_2)_6$-SH-3’(DNA2)

Apparatus. ECL emission was detected on an MPI-E multifunctional electrochemical and chemiluminescent analytical system (Xi’an Remax Electronic Science and Technology Co., Ltd., Xi’an, China). Cyclic voltammetry (CV), differential pulse voltammetry (DPV) and electrochemical impedance spectra (EIS) measurements were carried out with a CHI 660E electrochemistry workstation (Shanghai CH Instruments, China) at room temperature. The three-electrode system using an ITO electrode as the working electrode, Ag/AgCl (saturated KCl)

as the reference electrode and platinum wire as the counter electrode was used for all electrochemical tests. A scanning electron microscope (S-4800, Hitachi) was used to obtain the scanning electron micrographs (SEM). A JEOL-JEM 200 CX transmission electron microscope (Hitachi Instrument, Japan) was used to obtain the transmission electron micrographs (TEM). The confocal images were obtained by a TCS SP5 confocal laser microscope (Leica, Germany). The contact angle images were measured by a JC2000D1 static water contact angle (WCA) meter (Shanghai Zhongchen Instrument, China).

Synthesis of Water-Soluble CdS QDs. The CdS QDs were synthesized by a strategy already reported.[53] First, a $CdCl_2$ (20 mL, 20 mM) solution and MPA (86 μL) as a stabilizer were mixed at room temperature. After adjusting the pH of the system to 10 with 1 M NaOH, thioacetamide aqueous (20 mL, 20 mM) solution was added and stirred extensively for 30 min in air. Then, the mixture was refluxed at 80 °C for 10 h and purified overnight by dialysis in 25 °C deionized water. Finally, the resulting quantum dot solution was stored at 4 °C.

Production of Au-luminol−DNA2 Probes. First, red precipitate was obtained by centrifuging the prepared Au-luminol solution (12000 rcf, 10 min). Meanwhile, the sulfhydryl groups of the CEA aptamer (35 μL, 1 μM) were activated with TCEP (15 μL, 10 mM) for 0.5 h. Next, the activated aptamer solution was mixed with the prepared Au-luminol solution and then sonicated for 12 h to bind them through the Au-S bond. Finally, the resulting mixture was purified by centrifugation (10000 rcf, 5 min) and dispersed with 200 μL of PBS (0.1 M, pH=7.4).

Fabrication of the Ratiometric ECL Biosensor. All ITO electrodes (0.5 cm×3.0 cm) were ultrasonically cleaned in anhydrous acetone, ethanol and water for 20 min before use. PANI was polymerized to the ITO electrode surface by CV electropolymerization in 0.5 M H_2SO_4 solution

with 0.5 M aniline from - 0.2 V to + 0.8 V at 100 $mV \cdot s^{-1}$. Then, 50 μL of AuNP colloid was uniformly coated on the sensing surface for 30 min, and washed the electrode. Subsequently, the modified sensing surface was incubated in 0.1 M PBS (pH=7.4) including 2.0 mg/mL peptide and 10 mM TCEP for 12 h to attach the peptide to AuNPs via the Au-S bond. Next, the carboxy groups on CdS QDs were activated with 0.1 M EDC and 0.01 M NHS for 1 h, and then, the activated CdS QDs were coated on the modified electrode for 4 h so that they were connected to the peptide by amide bonds. Then, 50 μL of 1 μM DNA1 was dripped onto the modified electrode and connected to CdS QDs by amide bonds. Finally, 50 μL of Au-luminol-DNA2 probes prepared by the above process was applied to the electrode for hybridization for 2 h. The electrodes were cleaned three times using 0.1 M PBS (pH=7.4) for subsequent detection.

ECL Response of CEA. First, different amounts of CEA were dissolved into 0.1 M PBS (pH=7.4) and then used to soak the sensing interface for 4 h. Then, after washing the electrode with 0.1 M PBS (pH=7.4), the ECL response was tested in PBS (0.1 M, pH=8.0) including 0.1 M $K_2S_2O_8$ and 6.5 mM H_2O_2. The voltage range was from -1.5 to +0.8 V, and the voltage of the photomultiplier tube (PMT) was set at 800 V.

RESULTS AND DISCUSSION

Principle of the Ratiometric Anti-fouling ECL Biosensor. Scheme 1 shows the stepwise process to establish this ECL biosensor. CdS QDs were used as cathode ECL emitters, and the CEA aptamers (DNA2) modified by Au-luminol and quenching agent Cy5 fluorescent groups were used as anode ECL emitters. In the absence of CEA, the ERET between the fluorophore Cy5 and CdS QDs quenched the negative potential ECL response of CdS QDs, but the positive potential ECL response of Au-luminol can still be detected. Alternately, if CEA in present, it binds

to the substrate chain to detach Cy5 and Au-luminol from the sensing interface, which leads to a decrease of the positive potential ECL response and the recovery of the negative potential ECL response. According to the ratiometric ECL response under two different potentials, CEA was sensitively determined. More importantly, the introduction of anti-fouling peptide enabled the prepared biosensor to detect CEA in complex samples, such as human serum, with excellent selectivity.

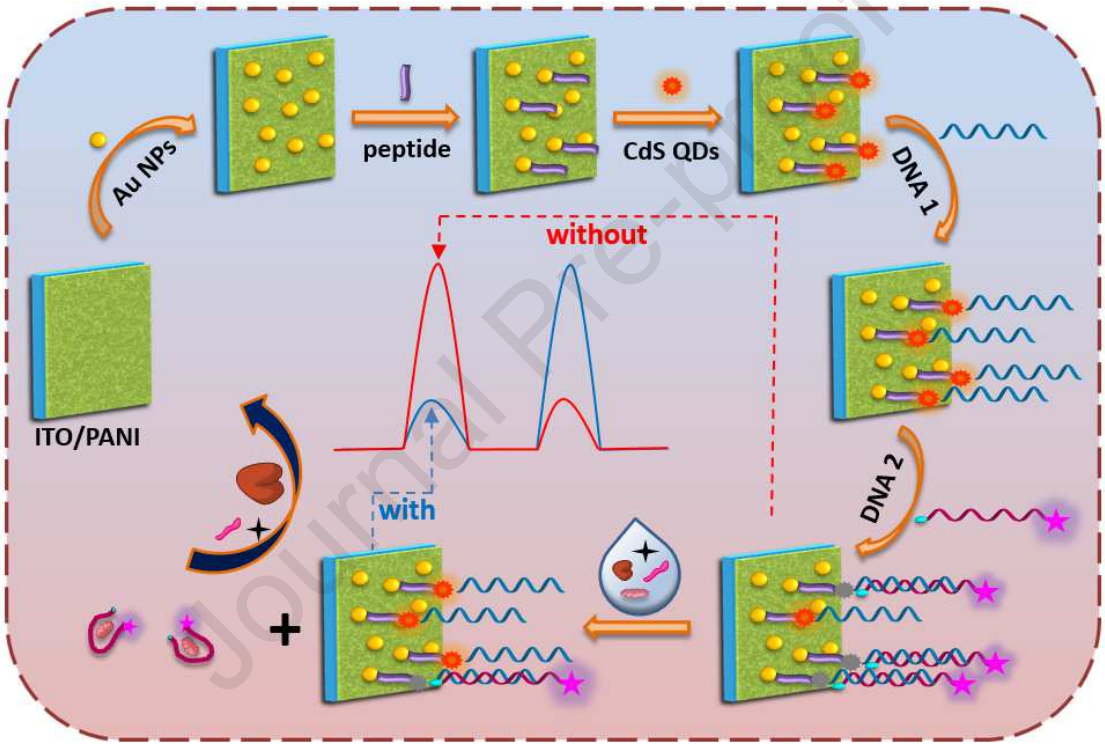

Scheme 1. Illustrative diagram of the anti-fouling ratiometric ECL system.

Morphological Characteristics of the Sensing Interfaces Developed. The morphologies of the step-by-step electrode surface were characterized by SEM (Figure 1). Figure 1A shows the surface morphology of the bare ITO. In contrast with the bare electrode, a new reticular structure can be observed on the surface of the ITO, which indicated that PANI was successfully deposited on the ITO (Figure 1B). The AuNPs were also very evenly coated on its mesh structure surface, as

shown in Figure 1C.

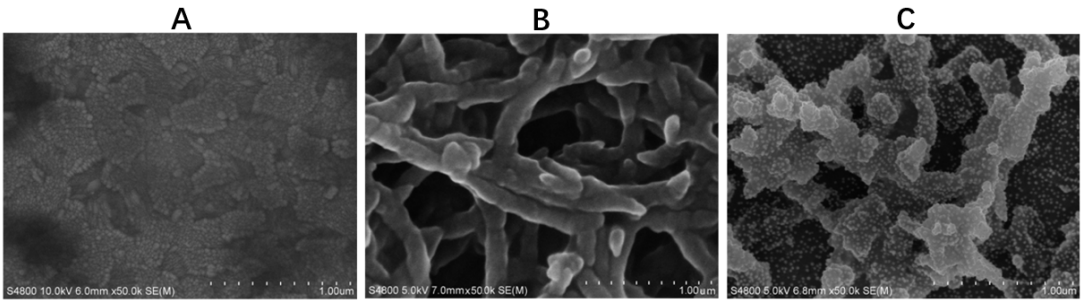

Figure 1. SEM characterization of the bare ITO (A), PANI/ITO (B), and AuNPs on PANI (C).

Features of AuNPs, Au-luminol and CdS QDs. The preparation of AuNPs and Au-luminol is detailed in Section 1 of the Supporting Information. The measurement and appearance of the synthesized Au-luminol, AuNPs and CdS QDs were observed by TEM. It can be observed from Figure S1A that, the average particle size of the prepared AuNPs was approximately 15 nm, the particle size of the Au-luminol (Figure S1B) was approximately 14 nm, and the particle size of the CdS QDs shown in Figure S1C was approximately 6 nm. As seen from the figure, they had very uniform particle sizes and great dispersibility.

The successful preparation of Au-luminol was certified by UV-vis spectra (Figure S2A). In the spectra, the characteristic absorption peaks of luminol solution were at 300 nm and 360 nm (curve a). The synthesized AuNPs showed an absorption peak at 525 nm (curve b). In contrast, the absorption peaks of Au-luminol were detected at 365 nm and 530 nm (curve c). The ECL responses and corresponding CV (inset) of CdS QDs and Au-luminol can be seen in Figure S2B. The ECL peak belonging to the CdS QDs at -1.5 V and the ECL peak belonging to the Au-luminol at 0.8 V can be observed in the figure. These results were in agreement with the conclusions already reported and demonstrated that Au-luminol and CdS QDs had been accurately synthesized.

CV and EIS of the Assembly Steps of the Developed Biosensor. The progressive construction approach of the detection platform was proven by CV and EIS. Two symmetric redox peaks can be seen (curve a) in Figure 2A due to the oxidation-reduction reaction of $[Fe(CN)_6]^{3-/4-}$ on the bare ITO. The current signal increased sequentially with the successive modification of the electrode by PANI (curve b) and AuNPs (curve c) because of their better conductivity and the increase of the effective area for the sensing interface. The peak current decreased sequentially (curve d, e, f) when the electrode was incubated with peptide, DNA1 and DNA2 in turn, which may be due to the insulation effect of the peptide and DNA.

EIS was used to further characterize the successful assembly of this biosensor (Figure 2B). Compared with bare ITO (curve a), the impedance (curve b) of the PANI-modified electrode was reduced, indicating that PANI was beneficial for electron transfer. After PANI/ITO was modified by AuNPs, the impedance decreased (curve c), which indicated that AuNPs had been successfully coated on the surface of PANI. After the continued incubation with peptide (curve d), DNA1 (curve e), and DNA2 (curve f), a continuous increase of RET was observed due to the hindrance of the electronic transmission of the signal probe. This result showed the same electron transfer trend as the CV curve, thus further proving the complete assembly of the sensing interface.

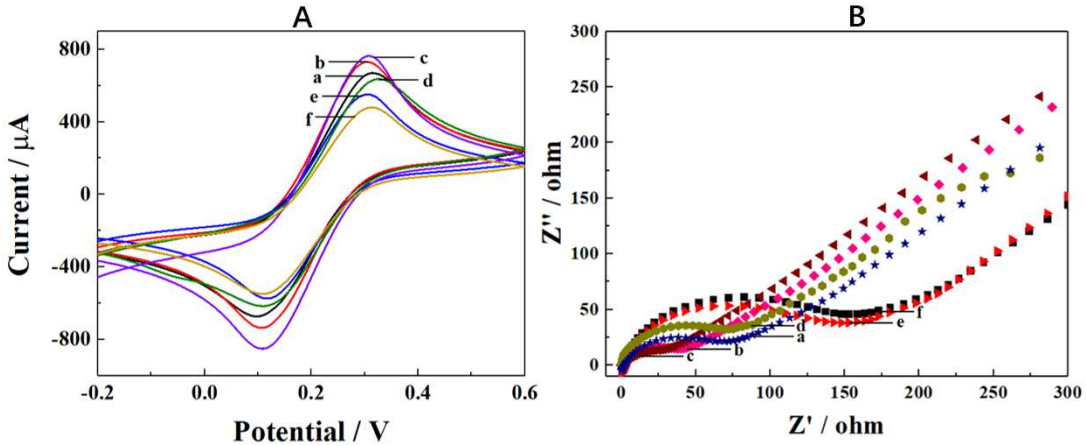

Figure 2. CV (A) and EIS (B) responses in 0.1 M PBS including 5.0 mM $[Fe(CN)_6]^{3-/4-}$ of the electrode construction process: (a) bare ITO, (b) PANI/ITO, (c) AuNPs/PANI/ITO, (d) peptide/AuNPs/PANI/ITO, (e) DNA1/peptide/AuNPs/PANI/ITO, and (f) Au-luminol-DNA2-Cy5/DNA1/peptide/AuNPs/PANI/ITO.

Anti-fouling Performance of the Modified Electrode. The basic requirements for anti-fouling performance are high hydrophilicity and electrical neutrality. It can be seen from Figure S3 that the Zeta potential of the peptide solution was almost 0.0 mV, which indicated that it was electrically neutral. The hydrophilicity of the peptide-modified biosensor interface was evaluated by the static water contact angle method (Figure S4 and Table S1). Compared with the bare ITO, the water contact angle of the sensing interface decreased gradually with the gradual assembly of PANI, AuNPs and peptide and decreased significantly after peptide modification.

After incubation of the sensor in different concentrations of FBS (V/V) for 30 min, the anti-fouling capability of the constructed sensing surface was further evaluated by comparing the changes in its DPV response (Figure 3). It can be seen that, even in 100% FBS, the DPV signal of the sensing interface with peptide incubation fluctuated only 14.3%. The experimental results show that the peptide-modified biosensor interface had good anti-fouling performance. The results were further verified by laser confocal imaging of fluorescein diacetate (FDA)-labeled cells (Figure S5). It can be seen that, compared with the electrodes modified with PANI and AuNPs, there are very few cells labeled with FDA on the peptide-modified interface, which further proves the anti-fouling performance of the sensor.

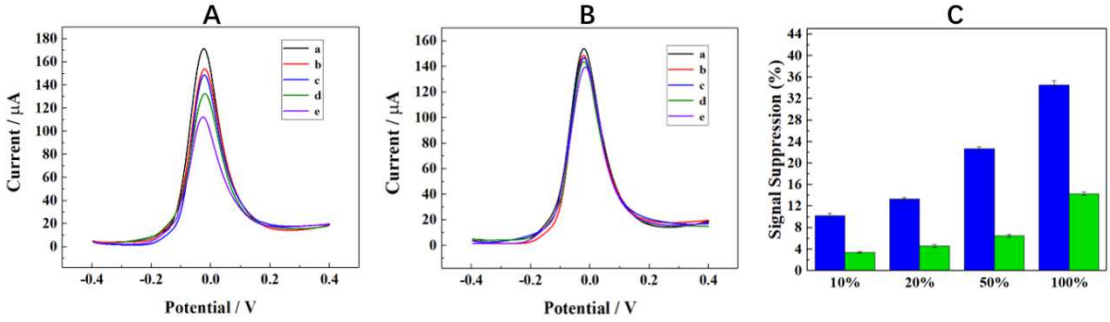

Figure 3. DPV characterizations of the biosensor modified without peptide (A) and with peptide (B) in different concentrations of FBS (0%, 10%, 20%, 50%, and 100%). (C) Anti-fouling characteristics of the biosensor modified without peptide (blue) and with peptide (green) in different concentrations of FBS.

Optimization of the Constructed Biosensor. The ECL signals from CdS QDs and Au-luminol in the constructed biosensor were affected by the amount of DNA1. This is because too much DNA1 could hinder the ECL signal response of CdS QDs, while too low an amount could limit the amount of Au-luminol-DNA2 probe and thus reduce the signal response of Au-luminol. The dose of DNA1 was optimized to make the two ECL signal molecules respond evenly (Figure S6).

ECL Performance of the Biosensor for CEA. Sensitive detection of different concentrations of CEA was achieved by an effective dual-wavelength ratiometric ECL system between CdS QDs and Au-luminol. As shown in Figure 4A, the negative potential ECL response from CdS QDs increased with rising concentrations of CEA, while the positive potential ECL response from Au-luminol decreased accordingly. Figure 4B shows that both the negative potential ECL response and positive potential ECL response were linearly correlated with the logarithm of C_{CEA}. To improve the accuracy of the detection, we determined the concentration of CEA by calculating the ratio of ECL_{CdS} to $ECL_{Au\text{-}luminol}$ and obtained a good linear correlation (Figure 4C). The regression equation can be represented as $lg(ECL_{CdS}/ECL_{Au\text{-}luminol}) = 0.23\ lgC_{CEA}$ (ng/mL)-0.3571 (R^2=0.993). The correlation coefficient of the ratiometric system is higher than that of single ECL probe systems, which indicates that the accuracy of detection is improved by using the ratio type signal. The detection limit (LOD) of the system was estimated to be 0.13 pg/mL (S/N=3). Compared with previously reported detection methods for CEA detection, our strategy exhibits a lower LOD (Table S2).

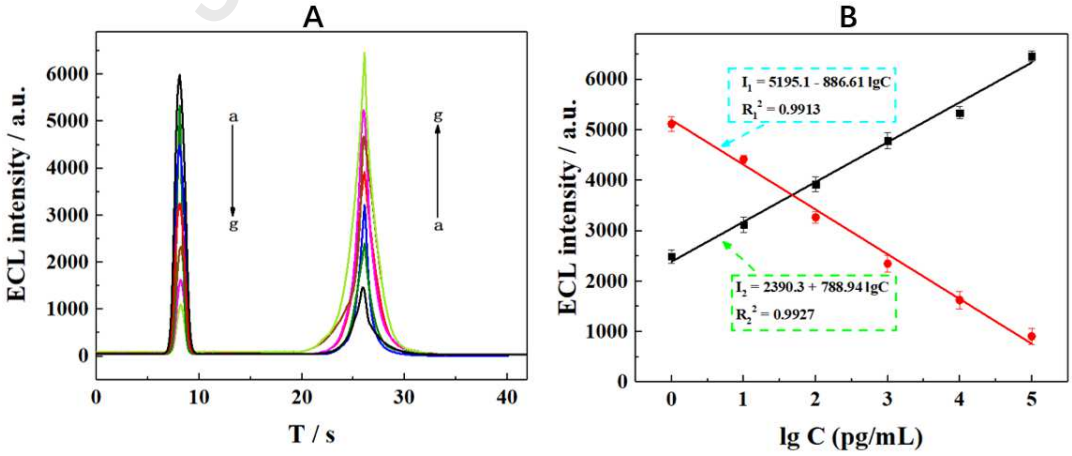

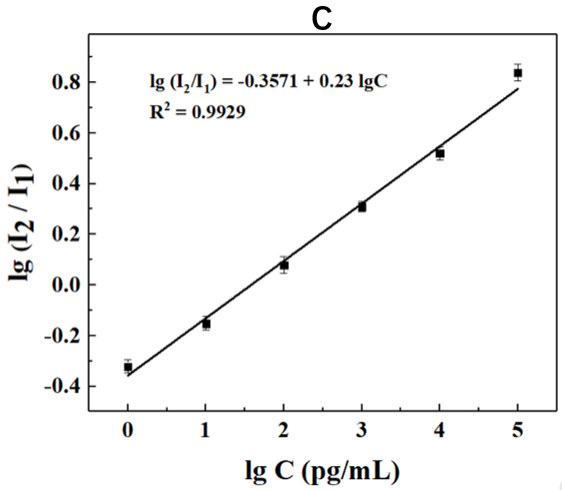

Figure 4. (A) ECL responses of this system for CEA standards with various concentrations: 0, 0.001, 0.01, 0.1, 1, 10, and 100 ng/mL (from a to g) in 0.1 M PBS with 0.1 M $K_2S_2O_8$ and 6.5 mM H_2O_2 at a pH of 8.0. (B) Calibration plot of $ECL_{Au\text{-}luminol}$ and the logarithmic value of C_{CEA} (red) and, $ECL_{CdS\ QDs}$ and the logarithmic value of C_{CEA} (black). (C) Calibration plot of the logarithmic value of $ECL_{Au\text{-}luminol}/ECL_{CdS\ QDs}$ and the logarithmic value of C_{CEA}.

Specificity and Stability of the System. To explore the specificity of the ECL detection platform for the target analyte, the responses of nontarget substances on the sensing platform were investigated. The biosensor was incubated with thrombin, AFP, hemoglobin, BSA, glucose, uric acid, Na^+, K^+, Cl^-, CEA and mixtures under the same conditions. As shown in Figure 5B, compared with interfering substances, the ECL response of CEA was significantly larger, while the ECL signal changes of other tested substances were very small. This result showed that the sensor has high selectivity to CEA. Next, the biosensor was subjected to CV scans to explore the stability of the constructed biosensor. It can be observed that the CV signal remains essentially unchanged after 25 cycles (Figure 5A). These results indicated that the constructed biosensor has satisfactory specificity and good stability.

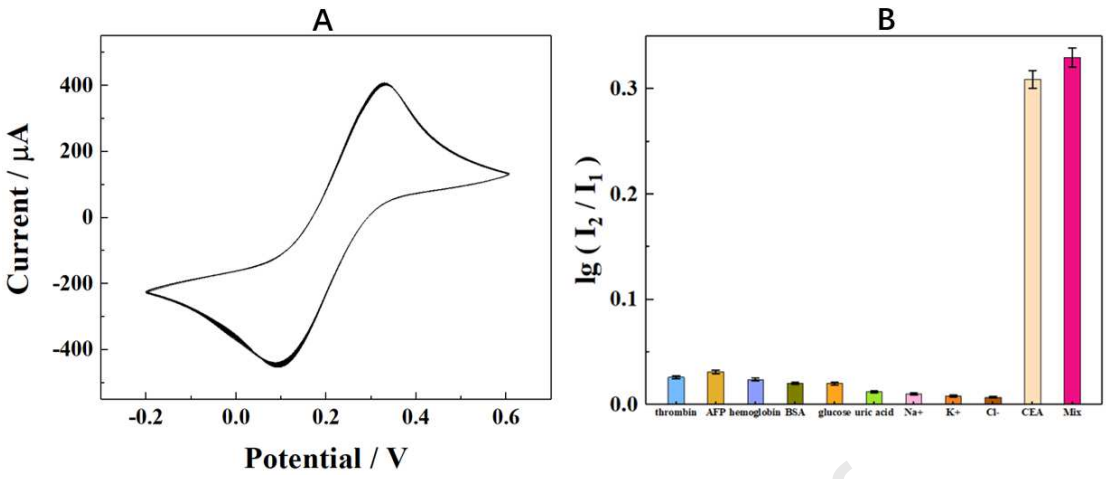

Figure 5. (A) Stability of the prepared biosensor in PBS (0.1 M, pH=7.4). (B) Selection performance of biosensors constructed after incubation with 1.0 ng/mL of CEA and 10.0 ng/mL of the following nontarget substances: thrombin, AFP, hemoglobin, BSA, glucose, uric acid, Na^+, K^+, and Cl^-.

Determination of CEA in Clinical Samples. To explore the practical potential of the immunosensor in complex matrices, human serum samples (from the Affiliated Hospital of Heze Medical College) containing three different concentrations of CEA were tested. As seen from the test results in Table 1, the relative error of this method is less than 5.6%. The results show that the constructed biosensor has the potential for practical application.

Table 1. Test Results for Actual Samples.

Sample	CEA detection of our strategy (ng/mL)[a]	CEA detection of the ECL method in the hospital (ng/mL)	Relative error (%)
1	3.93± 0.02	3.72	5.6
2	6.11±0.11	6.24	-2.1
3	16.15±0.05	16.03	0.7

[a] Average values of three measurements.

CONCLUSIONS

A ratiometric ECL sensor with anti-fouling ability based on ERET and anti-fouling peptide was

constructed. In this system, the negative potential ECL response of CdS QDs was quenched due to the ERET between the fluorescent group Cy5 and CdS QDs. After the target CEA combined with its aptamer and removed it from the sensing surface, the negative potential ECL response of CdS QDs recovered, and the positive potential ECL response of Au-luminol decreased. According to the analysis strategy of the ratiometric ECL signal under two different excitation potentials, the reliability and accuracy of the measured results were improved. The introduction of anti-fouling peptide caused the designed sensing interface to have good anti-fouling ability and provides a very attractive means for clinical diagnosis. The construction strategy of this biosensor is also expected to be extended to other accurate and anti-fouling biosensor designs.

ACKNOWLEDGMENTS

The authors greatly acknowledge support from the National Natural Science Foundation of China (Grants 21974075), the Taishan Scholar Program of Shandong Province of China (Grant ts20110829), and the Fund of Shandong Province Key Research and Development Program (2017GGX20121).

REFERENCES

[1] Torre, L. A.; Bray, F.; Siegel, R. L.; Ferlay, J.; Lortet-Tieulent, J., Jemal, A. *CA Cancer J Clin.* **2015**, 65, 87-108.

[2] Siegel, R. L.; Miller, K. D.; Jemal, A. *CA Cancer J Clin.* **2016**, 66, 7-30.

[3] Yang, F.; Zuo, X.; Li, Z.; Deng, W.; Shi, J.; Zhang, G.; Huang, Q.; Song, S.; Fan, C. *Adv. Mater.* **2014**, 26, 4671-4676.

[4] Qu, X.; Zhang, H.; Chen, H.; Aldalbahi, A.; Li, L.; Tian, Y.; Weitz, D. A.; Pei, H. *Anal. Chem.* **2017**, 89, 3468-3473.

[5] Benchimol, S.; Fuks, A.; Jothy, S.; Beauchemin, N.; Shirota, K.; Stanners, C. P. *Cell.* **1989**, 57, 327-334.

[6] Chen, X.; Ba, Y.; Ma, L.; Cai, X.; Yin, Y.; Wang, K.; Guo, J.; Zhang, Y.; Chen, J.; Guo, X.; Li, Q.; Li, X.; Wang, W.; Zhang, Y.; Wang, J.; Jiang, X.; Xiang, Y.; Xu, C.; Zheng, P.; Zhang, J.; Li, R.; Zhang, H.; Shang, X.; Gong, T.; Ning, G.; Wang, J.; Zen, K.;Zhang, J.; Zhang, C. Y. *Cell Res.* **2008**, 18, 997-1006.

[7] Miao, X.; Zou, S.; Zhang, H.; Ling, L. *Sens. Actuators, B.* **2014**, 191, 396-400.

[8] Hammarstrom, S. *Seminars in Cancer Biology*. **1999**, 9, 67-81.

[9] Altintas, Z.; Uludag, Y.; Gurbuz, Y.; Tothill, I. E. *Talanta.* **2011**, 86, 377-383.

[10] Liu, M.; Jia, C.; Huang, Y.; Lou, X.; Yao, S.; Jin, Q.; Zhao, J.; Xiang, J. *Analyst.* **2010**, 135, 327-331.

[11] Zhang, Y.; Ge, L.; Li, M.; Yan, M.; Ge, S.; Yu, J.; Song, X.; Cao, B. *Chem. Commun.* **2014**, 50, 1417-1419.

[12] Lin, Z.; Zhang, G.; Yang, W.; Qiu, B.; Chen, G. *Chem. Commun.* **2012**, 48, 9918-9920.

[13] Tian, J.; Zhou, L.; Zhao, Y.; Wang, Y.; Peng, Y.; Zhao, S. *Talanta.* **2012**, 92, 72-77.

[14] Wu, J.; Fu, Z.; Yan, F.; Ju, H. *TrAC Trends in Anal. Chem.* **2007**, 26, 679-688.

[15] Chen, B.; Hu, B.; Jiang, P.; He, M.; Peng, H.; Zhang, X. *Analyst.* **2011**, 136, 3934-3942.

[16] Liu, R.; Liu, X.; Tang, Y.; Wu, L.; Hou, X.; Lv, Y. *Anal. Chem.* **2011**, 83, 2330-2336.

[17] Zhang, Y. H.; Li, M. J.; Wang, H. J.; Yuan, R.; Wei, S.P. *Anal. Chem.* **2019**, 91, 10864-10869.

[18] Chen, Z.; Li, P.; Zhang, Z.; Zhai, X.; Liang, J.; Chen, Q.; Li, K.; Lin, G.; Liu, T.; Wu, Y. *Anal. Chem.* **2019**, 91, 5777-5785.

[19] Wang, D.; Li, Y.; Lin, Z.; Qiu, B.; Guo, L. *Anal. Chem*. **2015**, 87, 5966-5972.

[20] Yang, N.; Huang, Y.; Ding, G.; Fan, A. *Anal. Chem*. **2019**, 91, 4906-4912.

[21] Zhou, W.; Su, J.; Chai, Y.; Yuan, R.; Xiang, Y. *Biosens. Bioelectron.*.**2014**, 53, 494-498.

[22] Lai, W.; Wei, Q.; Zhuang, J.; Lu, M.; Tang, D. *Biosens. Bioelectron.* **2016**, 80, 249-256.

[23] Zhou, F.; Wang, M.; Yuan, L.; Cheng, Z.; Wu, Z.; Chen, H. *Analyst.* **2012**, 137, 1779-1784.

[24] Li, T.; Fan, Q.; Liu, T.; Zhu, X.; Zhao, J.; Li, G. *Biosens. Bioelectron.* **2010** 25, 2686-2689.

[25] Su, S.; Han, X.; Lu, Z.; Liu, W.; Zhu, D.; Chao, J.; Fan, C.; Wang, L.; Song, S.; Weng, L.; Wang, L. *ACS Appl. Mater. Interfaces.* **2017**, 9, 12773-12781.

[26] Song, C.; Min, L.; Zhou, N.; Yang, Y.; Yang, B.; Zhang, L.; Su, S.; Wang, L. *RSC Adv.* **2014**, 4, 41666-41669.

[27] Bai, X. R.; Wang, L. H.; Ren, J. Q.; Bai, X. W.; Zeng, L. W.; Shen, A, G.; Hu, J.M. *Anal. Chem*. **2019**, 91, 2955-2963.

[28] Ding, C. F.; Ge, Y.; Zhang, S. S. *Chem. Eur. J.* **2010**, 16, 10707-10714.

[29] Hu, L.; Xu, G. *Chem Soc Rev.* **2010**, 39, 3275-3304.

[30] Ding, C. F.; Wei, S.; Liu, H. T. *Chem. Eur. J*. **2012**, 18, 7263–7268.

[31] Amelia, M.; Lincheneau, C.; Silvi, S.; Credi, A. *Chem Soc Rev.* **2012**, 41, 5728-5743.

[32] Ding, C. F.; Zhang, W.; Wang, W.; Chen, Y. Y.; Li, X. Q. *Trends in Anal. Chem.* **2015**, 65, 137–150.

[33] Chen, Q.; Yu, S.; Zhang, D.; Zhang, W.; Zhang, H.; Zou, J.; Mao, Z.; Yuan, Y.; Gao, C.; Liu, R. *J Am Chem Soc*. **2019**, 141, 16772-16780.

[34] Gudipati, C. S.; Finlay, J. A.; Callow, J. A.; Callow, M. E.; Wooley, K. L. *Langmuir.* **2005**, 21, 3044-3053.

[35] Luo, X. L.; Xu, Q.; James, T.; Davis, J. J. *Anal. Chem.* **2014**, 86, 5553-5558.

[36] Li, Y.; Chen, R.; Feng, Y.; Sun, X.; Tang, L.; Takahashi, K.; Liu, P.; Wang, J. *Ind. Eng. Chem. Res.* **2019**, 58, 8016-8025.

[37] Xia, Y.; Adibnia, V.; Shan, C.; Huang, R.; Qi, W.; He, Z.; Xie, G.; Olszewski, M.; De Crescenzo, G.; Matyjaszewski, K.; Banquy, X.; Su, R. *Langmuir.* **2019**, 35, 15535-15542.

[38] Luo, X. L.; Xu, M. Y.; Freeman, C.; James, T.; Davis, J. J. *Anal. Chem*. **2013**, 85, 4129-4134.

[39] Wang, G. X.; Han, R.; Su, X. L.; Li, Y. N.; Xu, G. Y.; Luo, X. L. *Biosens Bioelectron.* **2017**, 92, 396-401.

[40] Liu, N. Z.; Hui, N.; Davis, J. J.; Luo, X. L. *ACS Sens.* **2018**, 3, 1210-1216.

[41] Liu, N. Z.; Song, J. Y.; Lu, Y. W.; Davis, J. J.; Gao. F. X.; Luo, X. L. *Anal. Chem.* **2019**, 91, 8334-8340.

[42] Hui, N.; Sun, X.; Niu, S.; Luo, X. *ACS Appl. Mater. Interfaces.* **2017**, 9, 2914-2923.

[43] Gaw, S. L.; Sakala, G.; Nir, S.; Saha, A.; Xu, Z. J.; Lee, P. S.; Reches, M. *Biomacromolecules.* **2018**, 19, 3620-3627.

[44] Zhang, X. Y.; Zhao, Y. Q.; Zhang, Y.; Wang, A.; Ding, X.; Li, Y.; Duan, S.; Ding, X.; Xu, F. J. *Biomacromolecules.* **2019**, 20, 4171-4179.

[45] Bae, C. W.; Toi, P. T.; Kim, B. Y.; Lee, W. I.; Lee, H. B.; Hanif, A.; Lee, E. H.; Lee, N. *ACS Appl. Mater. Interfaces.* **2019**, 11, 14567−14575.

[46] Wang, S. S.; Li, C. P.; Saqib, M.; Qi, G. H.; Ge, C. H.; Li, H. J.; Jin, Y. D. *Anal. Chem.* **2020**, 92, 845−852.

[47] Yang, Y.; Liang, Y.; Zhang, C. Y. *Anal. Chem*. **2017**, 89, 4055-4061.

[48] Doven, E. H.; Barbante, G. J.; Hogan, C. F.; Francis, P. S. *ChemPlusChem*. **2015**, 80, 456 – 470.

[49] Cheng, Y.; Huang, Y.; Lei, J.; Zhang, L.; Ju, H. *Anal. Chem*. **2014**, 86, 5158-5163.

[50] Li, Y. X.; Wang, L.; Ding, C. F.; Luo, X. L. *Biosens Bioelectron.* **2019**, 142, 111553.

[51] Ding, C. F.; Li, Y. X.; Wang, L.; Luo, X. L. *Anal. Chem.* **2019**, 91, 983-989.

[52] Ding, C. F.; Wang, X. Y.; Luo, X. L. *Anal. Chem*. **2019**, 91, 15846-15852.

[53] Han, E.; Ding, L.; Jin, S.; Ju, H. *Biosens Bioelectron.* **2011**, 26, 2500-2505.

1. Electrochemiluminescence resonance energy transfer (ERET) was used to construct the ratiometric ECL biosensor.
2. Ratiometric signal used in the ECL biosensor improved the accuracy of carcinoembryonic antigen detection.
3. Conductive polyaniline and gold nanoparticles enhanced the sensitivity of the modified electrode.
4. Antifouling peptide enabled this sensor to detect carcinoembryonic antigen in complex sample such as human serum.

Declaration of interests

☒ The authors declare that they have no known competing financial interests or personal relationships that could have appeared to influence the work reported in this paper.

☐The authors declare the following financial interests/personal relationships which may be considered as potential competing interests: